Hindawi
Shock and Vibration
Volume 2018, Article ID 9834629, 11 pages
https://doi.org/10.1155/2018/9834629

Research Article

Temperature Effects on Nonlinear Vibration Behaviors of Euler-Bernoulli Beams with Different Boundary Conditions

Yaobing Zhao and Chaohui Huang

College of Civil Engineering, Huaqiao University, Xiamen, Fujian 361021, China

Correspondence should be addressed to Yaobing Zhao; ybzhao@hqu.edu.cn

Received 14 January 2018; Revised 7 May 2018; Accepted 13 May 2018; Published 27 June 2018

Academic Editor: Pedro Galvín

This paper is concerned with temperature effects on the modeling and vibration characteristics of Euler-Bernoulli beams with symmetric and nonsymmetric boundary conditions. It is assumed that in the considered model the temperature increases/decreases instantly, and the temperature variation is uniformly distributed along the length and the cross-section. By using the extended Hamilton's principle, the mathematical model which takes into account thermal and mechanical loadings, represented by partial differential equations (PDEs), is established. The PDEs of the planar motion are discretized to a set of second-order ordinary differential equations by using the Galerkin method. As to three different boundary conditions, eigenvalue analyses are performed to obtain the close-form eigenvalue solutions. First four natural frequencies with thermal effects are investigated. By using the Lindstedt-Poincaré method and multiple scales method, the approximate solutions of the nonlinear free and forced vibrations (primary, super, and subharmonic resonances) are obtained. The influences of temperature variations on response amplitudes, the localisation of the resonance zones, and the stability of the steady-state solutions are investigated, through examining frequency response curves and excitation response curves. Numerical results show that response amplitudes, the number and the stability of nontrivial solutions, and the hardening-spring characteristics are all closely related to temperature changes. As to temperature effects on vibration behaviors of structures, different boundary conditions should be paid more attention.

1. Introduction

Due to the importance in many applications in many fields, such as the industrial, civil, mechanical, automotive, aerospace, and other structural systems, a flexible beam with nonlinear characteristics has attracted more attention in the past few years. The linear and nonlinear vibration characteristics have been investigated for many years and were reviewed, e.g., by Nayfeh and Mook [1], Nayfeh and Balachandran [2], Nayfeh and Pai [3], Luongo and Zulli [4], and Lacarbonara et al. [5].

On the one hand, it is noted that beams in compression are subjected to buckle, and once the beam buckles, the beam exhibits an initially deflected static equilibrium position and looks like an arch. Due to the initial curvature, the nonlinear vibration behaviors become much more complicated [6–8]. The nonlinear dynamics of buckled beams have been investigated by many researchers. As to these buckled and postbuckling beams, natural frequencies, mode shapes, nonlinear normal modes, and nonlinear resonance responses were investigated through theoretical and experimental methods [9–16]. The geometrically nonlinear vibration of an aluminium beam hinged at both ends was investigated experimentally by Ribeiro and Carneiro [17]. The nonlinear vibration analysis of a curved beam subjected to the uniform base harmonic excitation with both quadratic and cubic nonlinearities was investigated by Huang et al. [18].

On the other hand, in many applications, these structures are often subjected to vibration under thermal and dynamic loadings [19]. Temperature fields develop thermal stress due to the thermal expansion or contraction which influences the dynamic behavior of mechanical systems. The literature on thermal vibrations of mechanical structures is quite abundant; here, only a few papers are reviewed. The dynamic instability of a pinned beam subjected to an alternating magnetic field and thermal loads with the

nonlinear strain has been studied by Wu [20, 21], and effects of frequency ratio, loading factor and amplitude, damping factor, and temperature changes on the vibration behaviors have been illustrated. Manoach and Ribeiro [22, 23] studied geometrically nonlinear vibrations of moderately thick and curved beams under the combined action of mechanical and thermal loads. The coupled thermoelastic vibration characteristics of the axially moving beam were investigated by Guo et al. [24]. Treyssède [25] proposed an analytical model for the vibration analysis of horizontal beams that are self-weighted and thermally stressed. Moreover, due to the relatively high possible temperature variations in beams, Avsec and Oblak [26] have developed the mathematical model where fundamental thermomechanical properties of state are functions of temperature. Thermomechanical vibrations of a simply supported spring-mass-beam system were investigated analytically by Ghayesh et al. [27]. Three-dimensional nonlinear motion characteristics of the perfect and imperfect Timoshenko microbeams under mechanical and thermal forces have been examined numerically by Farokhi and Ghayesh [28]. Large amplitude vibrations and regular and chaotic oscillations of a Timoshenko beam under the influence of temperature were analysed by Warminska et al. [29, 30], and mechanical and thermal loadings have been discussed. Moreover, nonlinear vibration characteristics of cross-ply composite plates in thermal environments were investigated by Settimi et al. [31] and Saetta et al. [32]. Recently, based on Hamilton's principle, temperature effects on the vibration behaviors of the cable-stayed-beam by introducing two nondimensional factors were investigated by Zhao et al. [33]. The nonlinear free and forced vibration characteristics of the suspended cable were studied by Zhao et al. [34, 35].

Furthermore, the nonlinear vibration behavior of the system is closely related to its boundary conditions. For example, the nonlinear free and forced vibrations of a beam-mass system under five different boundary conditions were investigated by Ozkaya et al. [36]. Large amplitude vibrations of rectangular plates subjected to the radical harmonic excitation were investigated by Amabili [37], and three boundary conditions were considered. The nonlinear dynamic response of an inclined Timonshenko beam with different boundary conditions subjected to a varying mass with variable velocity was investigated by Mamandi et al. [38]. The nonlinear free vibrations of a two-layer elastic composite beam were studied by Lenci et al. [39], and different boundary conditions, both symmetric (e.g., free-free, fixed-fixed, and hinged-hinged) and nonsymmetric (e.g., free-fixed and hinged-fixed) with respect to the beam midpoint, were investigated. Furthermore, by using a unified approach, the planar nonlinear vibrations of the shear indeformable beams with either movable or immovable supports were investigated by Luongo et al. [40].

One of the motivations of this study is that changes in the vibration characteristics of the structure due to the damage may be smaller than changes in ones due to variations in temperature [41]. Therefore, an accurate mathematical model of the beam with thermal effects is necessary to predict its vibration characteristics. To the best of our knowledge, no specific study has addressed temperature effects on the nonlinear free and forced oscillations of the beam with different boundary conditions. The structure of the paper is organized as follows: in Section 2, the governing equations of an Euler-Bernoulli beam by using the extended Hamilton's principle are derived. In addition, the PDEs of the planar motion are discretized to the second-order ordinary equations via the Galerkin method. Considering three different boundary conditions, eigenvalue analyses are performed to obtain close-form eigenvalue solutions. Then, the Lindstedt-Poincaré method and multiple scales method are adopted to obtain the approximate solutions of the nonlinear free and forced resonance responses in Section 3. Some numerical results and discussions are given to illustrate the influences of temperature variations on response amplitudes, localisation of the resonance zones, and the stability of the nontrivial solutions in Section 4. Finally, at the end of the paper (Section 5), some conclusions are drawn.

2. Mathematics for Nonlinear Modeling

2.1. Equations of Motion. In this study, u and v denote the axial and transverse deflections of the beam, respectively, x is the distance along the undeflected beam, t is the time, L is the beam length, $m = \rho A$ is the beam's mass per unit, E is Young's modulus, A is the area of cross-section, I is the area moment of inertia, P is the applied axial compressive load, c_u and c_v are the viscous damping coefficients per unit length, ΔT is the temperature variation, and α is the thermal expansion coefficient.

The linear relation between the temperature variation and the stress-temperature coefficient γ is

$$\gamma(\Delta T) = E\alpha\Delta T, \tag{1}$$

and the nonlinear relation is expressed as [21]

$$\gamma(\Delta T) = E\alpha\Delta T + \widetilde{h}\alpha^2\Delta T^2. \tag{2}$$

Here, the first linear relation is adopted for the sake of simplicity. By assuming the Lagrangian strain as the strain measure and introducing temperature variations, the strain in the beam motion is obtained

$$\varepsilon = \frac{\partial u}{\partial x} + \frac{1}{2}\left(\frac{\partial v}{\partial x}\right)^2 - \frac{\gamma}{E}. \tag{3}$$

The extended Hamilton's principle is given by

$$\int_{t_1}^{t_2} \left[\delta W_e + \delta T - \delta U\right] \mathrm{d}t = 0, \tag{4}$$

where T is the kinetic energy, U is the elastic energy, and W_e is the work done by external loads on the system.

By using Hamilton's principle, one obtains [1, 20, 21]

$$\begin{aligned} &\rho A\frac{\partial^2 u}{\partial t^2} + c_u\frac{\partial u}{\partial t} \\ &\quad - A\frac{\partial}{\partial x}\left\{E\left[\frac{\partial u}{\partial x} + \frac{1}{2}\left(\frac{\partial v}{\partial x}\right)^2\right] - \gamma\right\} = 0, \end{aligned} \tag{5}$$

$$\rho A\frac{\partial^2 v}{\partial t^2}+c_v\frac{\partial v}{\partial t}+EI\frac{\partial^4 v}{\partial x^4}-A\frac{\partial}{\partial x}\left\{\frac{\partial v}{\partial x}\left\{E\left[\frac{\partial u}{\partial x}+\frac{1}{2}\left(\frac{\partial v}{\partial x}\right)^2\right]-\gamma\right\}\right\}+P\frac{\partial^2 v}{\partial x^2}=F(x)\cos(\Omega t), \tag{6}$$

where $F(x)$ is the spatial distribution of the harmonic load in the v direction and Ω is the excitation frequency.

Introducing the quasistatic assumptions, the acceleration and velocity terms in (5) are neglected [20, 21], and we obtain

$$A\frac{\partial}{\partial x}\left\{E\left[\frac{\partial u}{\partial x}+\frac{1}{2}\left(\frac{\partial v}{\partial x}\right)^2\right]-\gamma\right\}=0, \tag{7}$$

where

$$\frac{\partial u}{\partial x}+\frac{1}{2}\left(\frac{\partial v}{\partial x}\right)^2-\frac{\gamma}{E}=\text{constant}=\delta, \tag{8}$$

where δ is the average strain of the systems, and one obtains

$$\delta=\frac{1}{L}\int_0^L\left[\frac{\partial u}{\partial x}+\frac{1}{2}\left(\frac{\partial v}{\partial x}\right)^2-\frac{\gamma}{E}\right]dx=\frac{1}{2L}\int_0^L\left(\frac{\partial v}{\partial x}\right)^2dx-\frac{\gamma}{E}. \tag{9}$$

Therefore, substituting (9) into (6), we obtain the following nonlinear partial differential equation of motion without considering the torsion and shear rigidities:

$$EI\frac{\partial^4 v}{\partial x^4}+\rho A\frac{\partial^2 v}{\partial t^2}+c_v\frac{\partial v}{\partial t}+A\gamma\frac{\partial^2 v}{\partial x^2}+P\frac{\partial^2 v}{\partial x^2}=\frac{EA}{2L}\frac{\partial^2 v}{\partial x^2}\int_0^L\left(\frac{\partial v}{\partial x}\right)^2dx+F(x)\cos(\Omega t). \tag{10}$$

For the sake of simplicity, the following nondimensional quantities are introduced:

$$\begin{aligned}
v^*&=\frac{v}{L},\\
x^*&=\frac{x}{L},\\
t^*&=t\sqrt{\frac{P}{\rho AL^2}},\\
v_f&=\sqrt{\frac{EI}{PL^2}},\\
\gamma^*&=\frac{A\gamma}{P},\\
v_1&=\sqrt{\frac{EA}{P}},\\
F^*&=\frac{FL}{P},\\
\Omega^*&=\Omega\sqrt{\frac{\rho AL^2}{P}},\\
c_v^*&=c_v\sqrt{\frac{L^2}{\rho AP}}.
\end{aligned} \tag{11}$$

Substituting (11) into (10) and neglecting the asterisks, one obtains

$$v_f^2\frac{\partial^4 v}{\partial x^4}+\frac{\partial^2 v}{\partial t^2}+c_v\frac{\partial v}{\partial t}+\frac{\partial^2 v}{\partial x^2}+\gamma\frac{\partial^2 v}{\partial x^2}=\frac{1}{2}v_1^2\frac{\partial^2 v}{\partial x^2}\int_0^1\left(\frac{\partial v}{\partial x}\right)^2dx+F(x)\cos(\Omega t). \tag{12}$$

2.2. Linear Analysis. Dropping the damping, excitation, and nonlinear terms in (12), the following linear equation is obtained:

$$v_f^2\frac{\partial^4 v}{\partial x^4}+\frac{\partial^2 v}{\partial t^2}+(\gamma+1)\frac{\partial^2 v}{\partial x^2}=0, \tag{13}$$

and one lets

$$v(x,t)=\phi(x)e^{i\omega t}, \tag{14}$$

where i denotes the imaginary unit, $\phi(x)$ is the normalized undamped mode shape, and ω is the natural frequency.

Substituting (14) into (13), one obtains

$$v_f^2\frac{\partial^4 v}{\partial x^4}+(\gamma+1)\frac{\partial^2 v}{\partial x^2}-\omega^2\phi=0. \tag{15}$$

The corresponding eigenvalue equation is expressed as follows:

$$v_f^2D^4+(\gamma+1)D^2-\omega^2=0. \tag{16}$$

Accordingly, one lets

$$\begin{aligned}
\theta&=\sqrt{\frac{\sqrt{(1+\gamma)^2+4v_f^2\omega^2}+(1+\gamma)}{2v_f^2}},\\
\beta&=\sqrt{\frac{\sqrt{(1+\gamma)^2+4v_f^2\omega^2}-(1+\gamma)}{2v_f^2}}.
\end{aligned} \tag{17}$$

The homogeneous solution of (16) is given by

$$\phi(x)=c_1\cos(\theta x)+c_2\sin(\theta x)+c_3\cosh(\beta x)+c_4\sinh(\beta x). \tag{18}$$

In the following sections, three different symmetric and nonsymmetric boundary conditions are chosen and investigated: hinged-hinged, hinged-fixed, and fixed-fixed.

Case A (hinged-hinged). As to the hinged-hinged boundary conditions, we have

$$\phi(0) = \phi(1) = 0,$$
$$\left.\frac{\partial^2\phi}{\partial x^2}\right|_{x=0} = \left.\frac{\partial^2\phi}{\partial x^2}\right|_{x=1} = 0. \tag{19}$$

Substituting (19) into (18), we obtain the following coefficient matrix:

$$\begin{bmatrix} 1 & 0 & 1 & 0 \\ \cos(\theta) & \sin(\theta) & \cosh(\beta) & \sinh(\beta) \\ -\theta^2 & 0 & \beta^2 & 0 \\ -\theta^2\cos(\theta) & -\theta^2\sin(\theta) & \beta^3\cosh(\beta) & \beta^3\sinh(\beta) \end{bmatrix} \tag{20}$$

where the determinant of the coefficient matrix in (20) equals zero; we have

$$\left(\theta^2 + \beta^3\right)\sin(\theta)\sinh(\beta) = 0. \tag{21}$$

Hence, the natural frequency of the beam with hinged-hinged boundary conditions could be obtained by solving the following equation:

$$\sin(\theta) = 0, \tag{22}$$

and the corresponding mode shapes are

$$\phi_i(x) = C_i \sin(\theta_i), \tag{23}$$

where C_i is determined by normalization conditions.

Case B (hinged-fixed). As to the hinged-fixed boundary conditions, we have

$$\phi(0) = \phi(1) = 0,$$
$$\left.\frac{\partial^2\phi}{\partial x^2}\right|_{x=0} = \left.\frac{\partial\phi}{\partial x}\right|_{x=1} = 0. \tag{24}$$

Substituting (24) into (18), the coefficient matrix is

$$\begin{bmatrix} 1 & 0 & 1 & 0 \\ \cos(\theta) & \sin(\theta) & \cosh(\beta) & \sinh(\beta) \\ -\theta^2 & 0 & \beta^2 & 0 \\ -\theta\sin(\theta) & \theta\cos(\theta) & \beta\sinh(\beta) & \beta\cosh(\beta) \end{bmatrix} \tag{25}$$

Similarly, the following equation is obtained:

$$-\left(\theta^2 + \beta^2\right)\left[-\beta\cosh(\beta)\sin(\theta) + \theta\cos(\theta)\sinh(\beta)\right] = 0. \tag{26}$$

Hence, the natural frequency could be obtained by solving the following transcendental equation:

$$-\beta\cosh(\beta)\sin(\theta) + \theta\cos(\theta)\sinh(\beta) = 0, \tag{27}$$

with the following mode shapes:

$$\phi_i(x) = C_i\left[\frac{\sinh(\beta_i)\sin(\theta_i x) - \sin(\theta_i)\sinh(\beta_i x)}{\sin(\theta_i)}\right], \tag{28}$$

where C_i is also determined by normalization conditions.

Case C (fixed-fixed). As to the fixed-fixed boundary conditions, we have

$$\phi(0) = \phi(1) = 0,$$
$$\left.\frac{\partial\phi}{\partial x}\right|_{x=0} = \left.\frac{\partial\phi}{\partial x}\right|_{x=1} = 0. \tag{29}$$

Similarly, the coefficient matrix is

$$\begin{bmatrix} 1 & 0 & 1 & 0 \\ \cos(\theta) & \sin(\theta) & \cosh(\beta) & \sinh(\beta) \\ 0 & \theta & 0 & \beta \\ -\theta\sin(\theta) & \theta\cos(\theta) & \beta\sinh(\beta) & \beta\cosh(\beta) \end{bmatrix} \tag{30}$$

and we obtain the transcendental equation as

$$-2\theta\beta + 2\theta\beta\cos(\theta)\cosh(\beta) + \left(\theta^2 - \beta^2\right)\sin(\theta)\sinh(\beta) = 0, \tag{31}$$

where the natural frequency could be obtained, and the mode shapes are

$$\phi_i(x) = C_i\left[\left(\cosh(\beta_i x) - \cos(\theta_i x)\right) \cdot \frac{\beta_i\sin(\theta_i) - \theta_i\sinh(\beta_i)}{\theta_i\cosh(\beta_i) - \theta_i\cos(\theta_i)} + \sinh(\beta_i x) - \frac{\beta_i}{\theta_i} \cdot \sin(\theta_i)\right], \tag{32}$$

where C_i is also determined by normalization conditions.

2.3. Discrete Model. The Galerkin procedure is used to discretize (12) into a set of second-order ordinary differential equations

$$v(x,t) = \sum_{n=1}^{\infty}\phi_n(x)\,q_n(t), \tag{33}$$

where $q_n(t)$ is the generalized coordinate and $\phi_n(x)$ is the linear vibration mode shape.

Substituting (33) into (12), multiplying the result by $\phi_n(x)$, integrating the outcome over the domain, and finally using the orthonormality condition yield

$$\ddot{q}_n(t) + \omega_n^2 q_n(t) + 2\mu_n\dot{q}_n(t) + \sum_{i=1}^{\infty}\sum_{j=1}^{\infty}\sum_{k=1}^{\infty}\Gamma_{nijk}q_i(t)\,q_j(t)\,q_k(t) = f_n\cos(\Omega t), \tag{34}$$

where

$$\omega_n^2 = (\gamma+1)\int_0^1 \phi_n''(x)\,\phi_n(x)\,\mathrm{d}x + v_f^2\int_0^1 \phi_n''''(x)\,\phi_n(x)\,\mathrm{d}x, \tag{35}$$

$$\Gamma_{nijk} = -\frac{1}{2}v_f^2\int_0^1 \phi_i''(x)\,\phi_n(x)\left(\int_0^1 \phi_j(x)\,\phi_k(x)\,\mathrm{d}x\right)\mathrm{d}x, \tag{36}$$

$$f_n = \int_0^1 F(x)\,\phi_n(x)\,\mathrm{d}x, \tag{37}$$

$$\mu_n = \frac{1}{2}\int_0^1 c_v\phi_n(x)\,\mathrm{d}x. \tag{38}$$

3. Perturbation Analysis

Perturbation methods are used to investigate the nonlinear free, primary, super, and subharmonic resonance responses of the beam with thermal effects subjected to the planar excitation, and no internal resonance is considered in this study. For the sake of simplicity, only the single-mode discretization equation is considered

$$\ddot{q}_n(t) + \omega_n^2 q_n(t) + 2\mu_n\dot{q}_n(t) + \Gamma_{nnnn}q_n^3(t) = f_n\cos(\Omega t). \tag{39}$$

3.1. Nonlinear Free Vibration. This section begins with the approximate series solutions for the nonlinear free vibrations obtained with the Lindstedt-Poincaré method [42].

Firstly, a new independent variable $\widetilde{t}$ is introduced, which is

$$\widetilde{t} = \omega_n t, \tag{40}$$

where ω_n is the natural frequency.

Therefore, by neglecting the damping and forcing terms, (39) is transformed into

$$\ddot{q}_n + q_n + \frac{\Gamma_{nnnn}}{\omega_n^2}q_n^3 = 0, \tag{41}$$

where the coefficient of the linear term is equal to unity since the time is nondimensionalized with respect to the linear vibration frequency.

By assuming an expansion for $q_n = \varepsilon\widetilde{q_n}$ (where ε is a small finite nondimensional parameter) and omitting the tilde, we obtain

$$\ddot{q}_n + q_n + \varepsilon^2\frac{\Gamma_{nnnn}}{\omega_n^2}q_n^3 = 0. \tag{42}$$

Following the method of Lindstedt-Poincaré, we seek the fourth-order approximate solution to (42) by letting

$$q_n(\widetilde{t};\varepsilon) = \sum_{m=0}^{4}\varepsilon^m q_{nm}(t), \tag{43}$$

and a strained time coordinate τ is introduced

$$\tau = \left(1 + \sum_{m=1}^{4}\varepsilon^m\alpha_m\right)\widetilde{t}. \tag{44}$$

Then, we could obtain the relation between the nonlinear frequency Ω_n and the linear one ω_n as follows:

$$\frac{\Omega_n - \omega_n}{\omega_n} = \sum_{m=1}^{4}\varepsilon^m\alpha_m. \tag{45}$$

Substituting (43)-(44) into (42) and equating the coefficients ε^m on both sides, the nonlinear ordinary equations are reduced to a set of linearized equations. Then, the polar form is introduced and the secular terms are set to zero. Finally, the series solutions of q_{nm} and α_m are obtained, based on which the fourth-order series solutions of the frequency amplitude relationship and displacement are as follows:

$$\Omega_n = \omega_n\left[1 + \frac{3}{8}\frac{\Gamma_{nnnn}}{\omega_n^2}a^2 - \frac{15}{256}\frac{\Gamma_{nnnn}^2}{\omega_n^4}a^4\right], \tag{46}$$

where a is the actual nondimensional response amplitude.

3.2. Primary Resonances. First of all, we order the damping, excitation, and nonlinearity term as follows [43]:

$$2\mu_n\dot{q}_n(t) = 2\varepsilon\mu_n\dot{q}_n(t),\quad f_n\cos(\Omega_n t) = \varepsilon f_n\cos(\Omega_n t),\quad \Gamma_{nnnn}\dot{q}_n^3(t) = \varepsilon\Gamma_{nnnn}\dot{q}_n^3(t). \tag{47}$$

Substituting (47) into (39), the governing equation becomes

$$\ddot{q}_n(t) + \omega_n^2 q_n(t) + 2\varepsilon\mu_n\dot{q}_n(t) + \varepsilon\Gamma_{nnnn}q_n^3(t) = \varepsilon f_n\cos(\Omega t). \tag{48}$$

In the case of the primary resonance, we introduce a detuning parameter σ_n, which quantitatively describes the nearness of Ω_n to ω_n

$$\Omega_n = \omega_n + \varepsilon\sigma_n, \tag{49}$$

where ε is a small finite parameter.

We express the solution in terms of different time scales as

$$q_n(t;\varepsilon) = u_{n0}(T_0,T_1) + \varepsilon u_{n1}(T_0,T_1) + \cdots \tag{50}$$

where $T_0 = t$ and $T_1 = \varepsilon t$.

Substituting (49)-(50) into (48), equating the coefficients of ε^0 and ε^1 on both sides, following the method of multiple scales, finally the frequency response equation is obtained

$$\sigma_n = \frac{3}{8}\frac{\Gamma_{nnnn}}{\omega_n}a_n^2 \pm \sqrt{\frac{f_n^2}{4\omega_n^2 a_n^2} - \mu_n^2}, \tag{51}$$

where a_n is the actual nondimensional response amplitude.

Therefore, the first approximation to the steady-state solution is obtained

$$q_n(t) = a_n\cos(\Omega_n t - \gamma_n) + O(\varepsilon), \tag{52}$$

where t is the actual time scale and γ_n is the phase.

Table 1: Physical parameters and material properties.

Parameter	Physical meaning	Value	Unit
ρ	density	7781	kg/m^3
L	length	2.032	m
E	Young's modulus	207	GPa
A	area of cross-section	2.581×10^{-3}	m^2
α	thermal expansion coefficient	1.0×10^{-5}	/°C
P	axial load	11.281	kN
I	area moment of inertia	5.550×10^{-7}	m^4

3.3. Subharmonic Resonances. In order to investigate the subharmonic resonance, a detuning parameter σ_n is introduced

$$\Omega_n = 3\omega_n + \varepsilon\sigma_n, \tag{53}$$

where ε is a small but finite parameter.

Similarly, the frequency response equation can be obtained by using the multiple scales method

$$9\mu_n^2 + \left(\sigma_n - \frac{9\Gamma_{nnnn}\Lambda_n^2}{\omega_n} - \frac{9\Gamma_{nnnn}}{8\omega_n}a_n^2\right)^2 = \frac{81\Gamma_{nnnn}^2\Lambda_n^2}{16\omega_n^2}a_n^2, \tag{54}$$

where

$$\Lambda_n = \frac{1}{2}\frac{f_n}{\omega_n^2 - \Omega_n^2}. \tag{55}$$

The first approximation to the steady-state solution is given by

$$q_n(t) = a_n \cos\left[\frac{1}{3}(\Omega_n t - \gamma_n)\right] + \frac{f_n}{\omega_n^2 - \Omega_n^2}\cos(\Omega_n t) + O(\varepsilon), \tag{56}$$

where a_n is the actual nondimensional response amplitude, t is the actual time scale, and γ_n is the phase.

3.4. Super Harmonic Resonances. In this case, to express the nearness of Ω_n to $(1/3)\omega_n$, we also introduce the detuning parameter σ_n defined by

$$3\Omega_n = \omega_n + \varepsilon\sigma_n, \tag{57}$$

where ε is a small but finite parameter.

Following the step of the multiple scales method, a frequency response equation can be obtained

$$\sigma_n = 3\frac{\Gamma_{nnnn}\Lambda_n^2}{\omega_n} + \frac{3\Gamma_{nnnn}}{8\omega_n}a_n^2 \pm \sqrt{\frac{\Gamma_{nnnn}^2\Lambda_n^6}{\omega_n^2 a_n^2} - \mu_n^2}, \tag{58}$$

where

$$\Lambda_n = \frac{1}{2}\frac{f_n}{\omega_n^2 - \Omega_n^2}. \tag{59}$$

Therefore, the first approximation in this case is obtained

$$q_n(t) = a_n \cos(3\Omega_n t - \gamma_n) + \frac{f_n}{\omega_n^2 - \Omega_n^2}\cos(\Omega_n t) + O(\varepsilon), \tag{60}$$

where a_n is the actual nondimensional response amplitude, t is the actual time scale, and γ_n is the phase.

4. Numerical Examples and Discussions

In the following numerical analysis, material properties and physical parameters of the beam are chosen in Table 1. The nondimensional temperature variation factor γ is chosen as $[-1.0, +1.0]$, and the corresponding dimensional temperature variation ΔT is [−20.83°C, +20.83°C]. Moreover, the nondimensional factor ν_f in (11) is 0.5 in this study.

4.1. Natural Frequencies. By using the numerical method, the transcendental equations (see (22), (27), and (31)) can be solved, and the corresponding natural frequencies are obtained. In order to investigate temperature effects on natural frequencies with different boundary conditions, a frequency variation factor R_ω is defined

$$R_\omega = \frac{\omega_{\Delta T} - \omega_0}{\omega_0}, \tag{61}$$

where $\omega_{\Delta T}$ and ω_0 are the natural frequencies with and without thermal effects, respectively.

Figure 1 shows effects of temperature variations on the first four mode frequencies in the case of three different boundary conditions. As shown in these figures, with the increase (decrease) in the temperature, the mode frequencies all decrease (increase). In previous studies, it is shown that an increase in temperature leads to a decrease in natural frequencies [41], and the conclusion in this study is in good agreement with some of the previous findings.

Furthermore, the changing of natural frequencies with temperature was found to be dependent on the order of the mode and boundary conditions. With the increase of the order, the natural frequency becomes less sensitive to the temperature variation. To be more specific, in the case of $\gamma = +1.0$, as to three different boundary conditions, the variation factors R_ω of these first order mode frequencies are 43.6% (hinged-hinged), 13.0% (hinged-fixed), and 5.7%

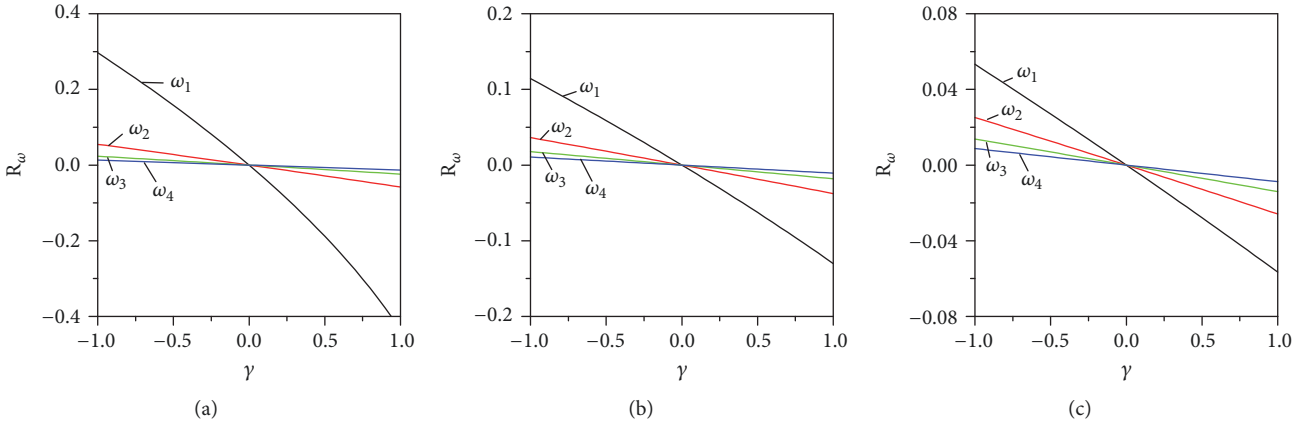

FIGURE 1: Temperature effects on the first four natural frequencies: (a) hinged-hinged; (b) hinged-fixed; (c) fixed-fixed.

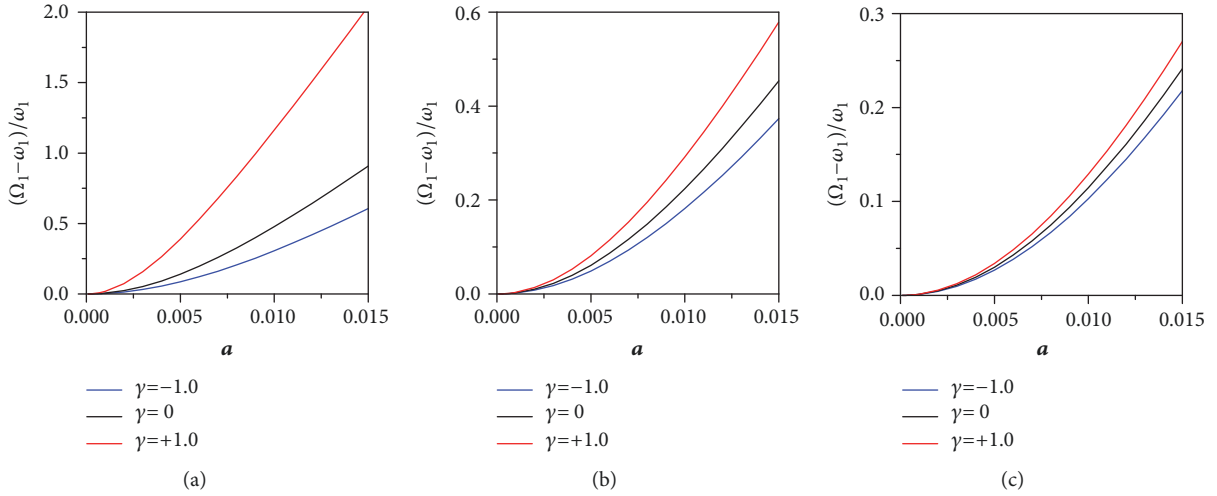

FIGURE 2: Frequency response curves of nonlinear free vibrations: (a) hinged-hinged; (b) hinged-fixed; (c) fixed-fixed.

(fixed-fixed), respectively. However, as to the fourth-order mode frequencies, the corresponding variation ratios R_ω are 1.3%, 1.1%, and 0.9%, respectively. Moreover, we can observe a slightly higher sensitivity to warming than cooling in the case of the hinged-hinged boundary condition, as shown in Figure 1(a). However, in the case of the fixed-fixed boundary condition (Figure 1(c)), the asymmetry phenomenon between the cooling and warming conditions almost disappears. It is concluded that temperature effects are very closely related to the boundary conditions, and the natural frequency decreases with an increase in temperature. In addition, it should be pointed out that, as to these three cases, temperature effects on mode shapes can be negligible.

4.2. Nonlinear Free and Forced Vibrations. Neglecting the damping and excitation terms, the nonlinear free vibrations of the beam with thermal effects are investigated. Figure 2 illustrates temperature effects on the nonlinear free vibration behaviors in the case of three different boundary conditions. Frequency response curves all show the hardening-spring characteristics due to the cubic nonlinearity term. The hardening behavior tends to increase for a positive temperature change and to decrease for a negative one. Moreover, with the enhancement of the constraint conditions (from hinged-hinged, hinged-fixed to fixed-fixed), temperature effects on the vibration behaviors are reduced.

Temperature effects on the nonlinear responses to the primary, super, and subharmonic excitations are studied in the following in terms of frequency response curves and excitation response curves, respectively. Moreover, by using the multiple scales method, the stability of these solutions is determined by examining the eigenvalues of the Jacobian matrix evaluated at the equilibrium point.

In the nonlinear resonant cases, the nondimensional excitation amplitude is chosen as 0.05, and the nondimensional damping coefficient is assumed to be independent of the temperature variation ($\mu_n = 0.01$). Figure 3 shows temperature effects on frequency response curves of the primary resonance, and three different boundary conditions are considered. There are almost three steady-state solutions: one unstable, plotted in dashed lines, and two stable, of low and high amplitudes, plotted in continuous lines, respectively. The stable solution is physically determined by the initial condition of the system finally. In the primary resonance,

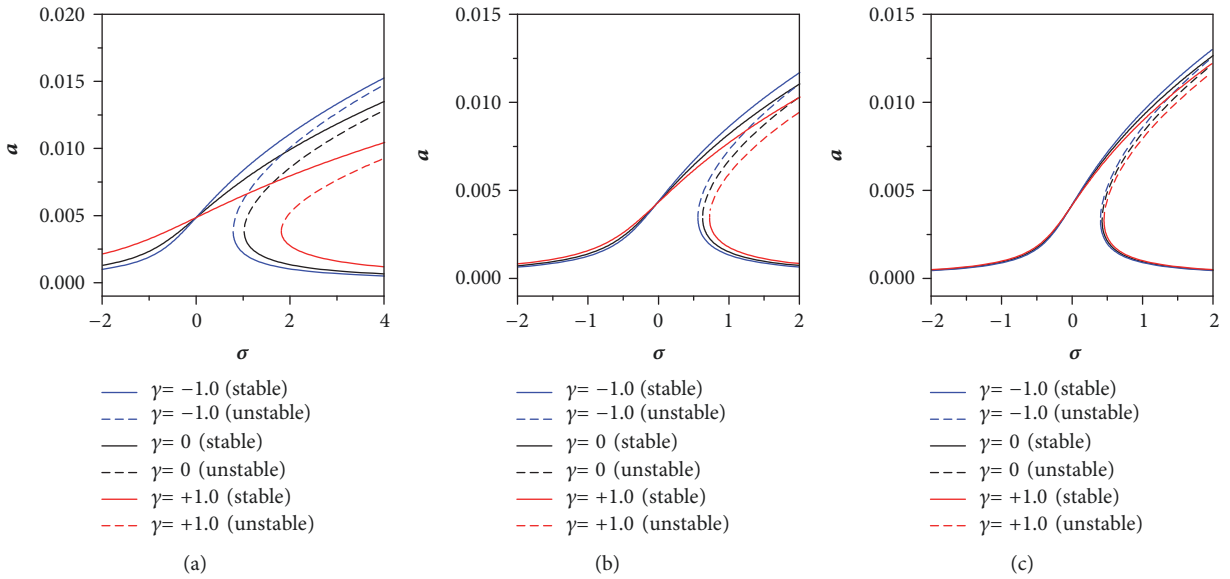

Figure 3: Frequency response curves of primary resonances: (a) hinged-hinged; (b) hinged-fixed; (c) fixed-fixed.

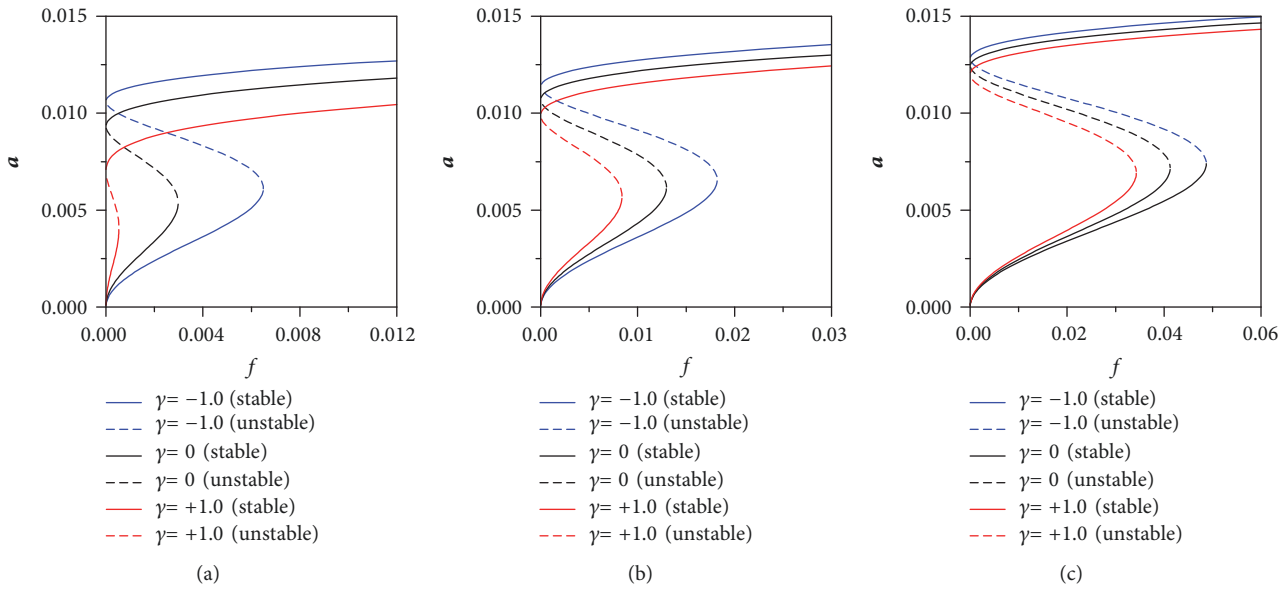

Figure 4: Excitation response curves of primary resonances ($\sigma = 2.0$): (a) hinged-hinged; (b) hinged-fixed; (c) fixed-fixed.

the system exhibits the hardening-spring behavior due to the cubic nonlinearity term, and all these curves bend to the right side. As to the hinged-hinged boundary condition as shown in Figure 3(a), temperature effects are obvious. Specifically, in the range of the large response amplitude, the response amplitude decreases with the increase in the temperature. On the contrary, as to the small response amplitude, the response amplitude increases with the increase in the temperature. As to the hinged-fixed and fixed-fixed boundary conditions, the temperature effect on the frequency response curves is negligible in the range of small response amplitudes. However, as to the large response amplitudes, the curve bends to the right more in the warming condition. As to the boundary conditions from hinged-hinged to fixed-fixed, it is noted that the temperature effect on the resonance characters is reduced.

Figure 4 shows the variation of the response amplitude with the excitation amplitude in the case of the primary resonance under three boundary conditions. Actually, it is known that, depending on the value of detuning parameter σ, some curves are multivalued while others are single-value. In this study, only the case of $\sigma = 2.0$ is investigated. As shown in these figures, the multivaluedness of frequency response curves due to the nonlinearity leads to the jump phenomenon in the excitation response curves. There are significant quantitative changes of these curves due to temperature variations. Moreover, it is noted that, in the range of large and small response amplitudes, temperature

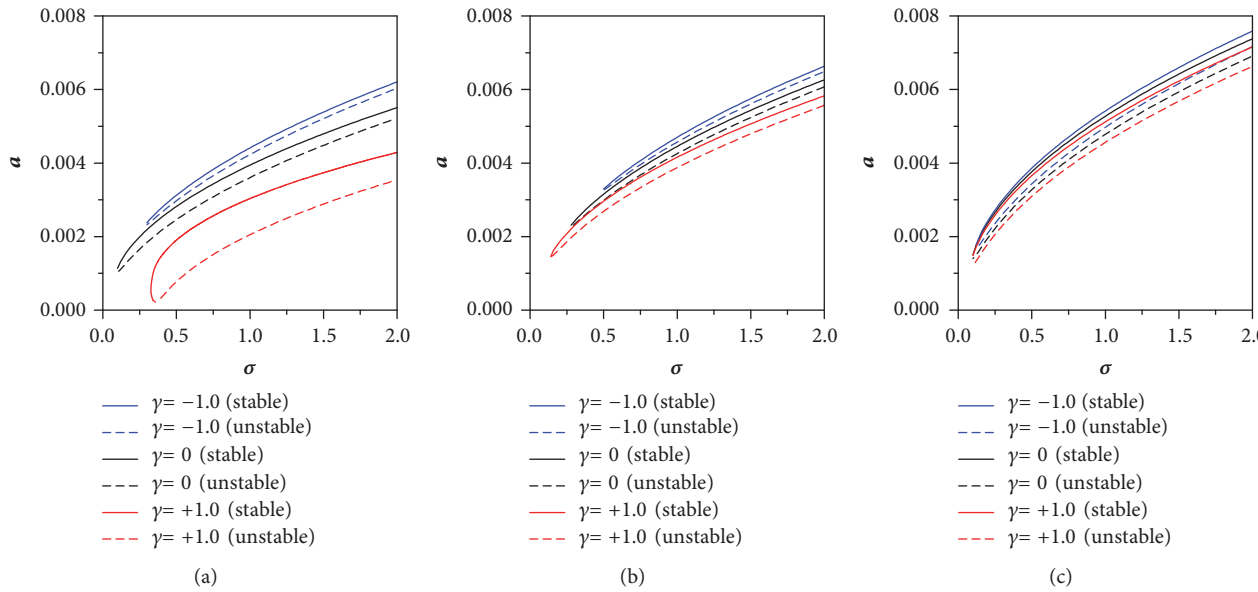

Figure 5: Frequency response curves of subharmonic resonances: (a) hinged-hinged; (b) hinged-fixed; (c) fixed-fixed.

effects are different. Specifically, as to the small response amplitude, with the increase in the temperature, the response amplitude increases slightly. On the contrary, as to the large one, the response amplitude decreases significantly in the same condition.

Temperature effects on the subharmonic resonance are shown in Figure 5. In this case, the stable trivial solution ($a_n \equiv 0$) is not shown, and only two nontrivial solutions are studied, in which one is stable and another is unstable. It is noted that there is no jump phenomenon in the case of the subharmonic resonance. As shown in Figure 5(a), as to the hinged-hinged boundary condition, the temperature effect is the most visible, and the threshold response amplitude decreases with an increase temperature and increases with a decrease one. The same conclusion could be observed from the Figure 5(b), in the case of the hinged-fixed boundary condition. In the last case (Figure 5(c)), it is shown that the temperature effect on the frequency response curve is not obvious.

Moreover, excitation response curves of the subharmonic resonance in the case of the hinged-hinged boundary condition when $\sigma = 2.0$ are illustrated in Figure 6. It is noted that there are significant quantitative changes of these curves due to temperature variations. Considering the temperature variations, the same response amplitude a is induced by very different excitation amplitude f. Moreover, under the excitation with the same amplitude f, very different response amplitudes are obtained due to the temperature variations.

Figure 7 illustrates temperature effects on frequency response curves in the case of the super harmonic resonance, and three boundary conditions are also included. Due to the effect of the cubic nonlinearity, the system exhibits the hardening behavior. Generally, as same as the previous resonant cases, the hardening behavior also increases with

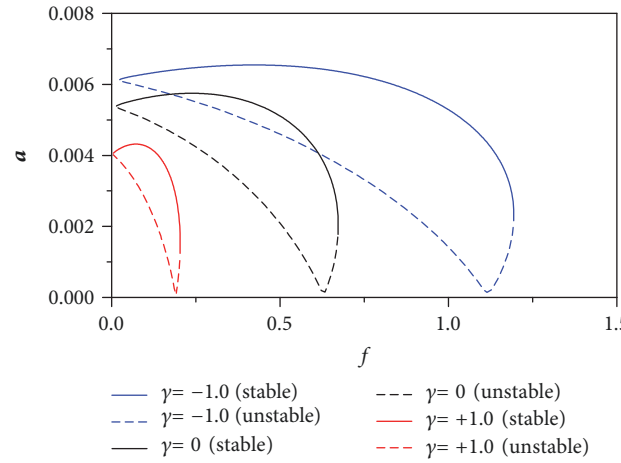

Figure 6: Excitation response curves of subharmonic resonances in the case of hinged-hinged boundary condition ($\sigma = 2.0$).

an increase in temperature and decreases with a decrease in temperature. However, it should be pointed out that, in the case of the super harmonic resonance (Figure 7(a)), no unstable solution is obtained and no jump phenomenon is observed in the warming condition ($\gamma = +1.0$). As shown in Figure 7(b), with the increase in the temperature, the curve bends to the right more and the system exhibits stronger hardening-spring behavior. It should be pointed out that, in the case of the cooling condition ($\gamma = -1.0$), the peak value of the frequency response curve decreases significantly. In the last case as shown in Figure 7(c), as to the system with fixed-fixed boundary condition, temperature effects on the super harmonic resonance are much more obvious than the ones on the primary resonance, and frequency response curves are shifted to the right more with the increase in temperature.

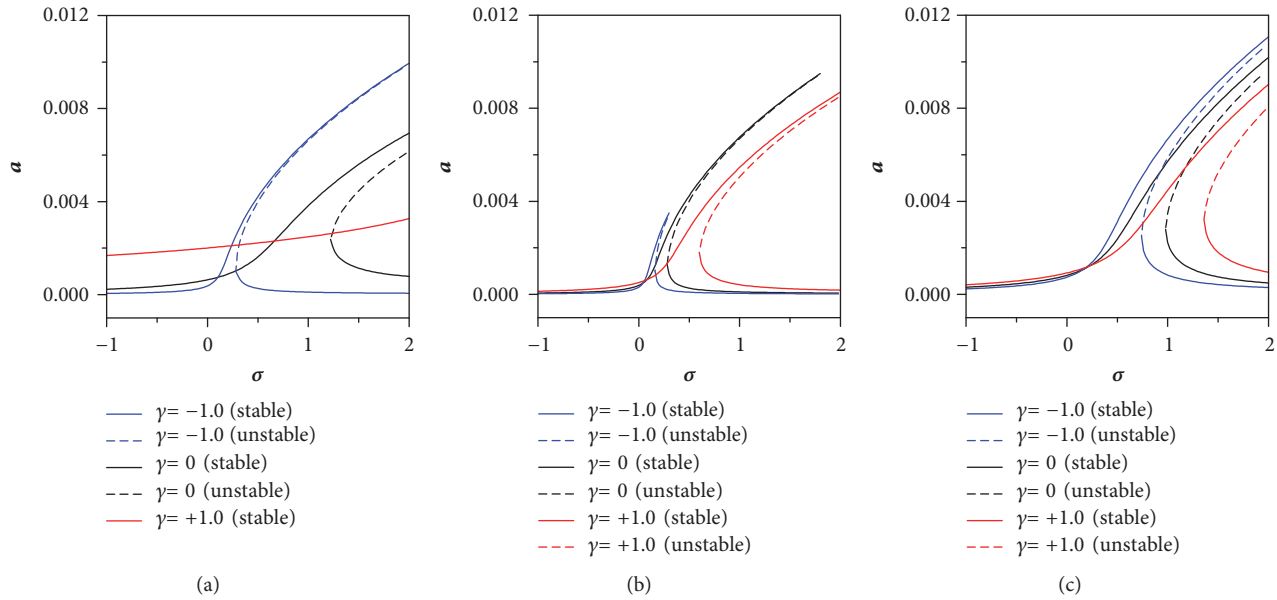

Figure 7: Frequency response curves of super harmonic resonances: (a) hinged-hinged; (b) hinged-fixed; (c) fixed-fixed.

5. Summary and Conclusions

A positive (resp., negative) temperature change does decrease (resp., increase) natural frequencies, and temperature effects on mode shapes can be negligible. Temperature effects on the vibration behaviors are closely related to the mode order and boundary conditions, and one can observe a slightly higher sensitivity to warming than cooling. As to the nonlinear vibration characteristics with thermal effects, no matter the primary, super, or subharmonic resonant cases, the system exhibits the hardening-spring behavior due to the cubic nonlinearity term. The hardening behavior increases with an increase in temperature, and it decreases with a decrease in temperature. Only some quantitative changes are observed due to the temperature changes by examining the frequency response curves and excitation response curves. The response amplitude, the stability, and the number of the nontrivial solutions and the range of the resonance response are all closely related to temperature variations. Moreover, as to temperature effects on vibration characteristics of the beam, different symmetric and nonsymmetric boundary conditions should be paid more attention.

Data Availability

The data used to support the findings of this study are available from the corresponding author upon request.

Conflicts of Interest

The authors declare that there are no conflicts of interest regarding the publication of this paper.

Acknowledgments

The research described in this paper was financially supported by the National Natural Science Foundation of China (11602089) and the Promotion Program for Young and Middle-Aged Teacher in Science and Technology Research of Huaqiao University (ZQN-YX505).

References

[1] A. H. Nayfeh and D. T. Mook, *Nonlinear Oscillations*, John Wiley & Sons, New York, NY, USA, 1979.

[2] A. H. Nayfeh and B. Balachandran, *Applied Nonlinear Dynamics: Analytical, Computational and Experimental Methods*, Wiley Series in Nonlinear Science, John Wiley & Sons, 1995.

[3] A. H. Nayfeh and P. F. Pai, *Linear and Nonlinear Structural Mechanics*, Wiley-Interscience, New York, NY, USA, 2004.

[4] A. Luongo and D. Zulli, *Mathematical Models of Beams and Cables*, John Wiley & Sons, Inc., Hoboken, USA, 2013.

[5] W. Lacarbonara, *Nonlinear structural mechanics*, Springer, Berlin, 2013.

[6] D. Zulli, R. Alaggio, and F. Benedettini, "Non-linear dynamics of curved beams. Part 1: Formulation," *International Journal of Non-Linear Mechanics*, vol. 44, no. 6, pp. 623–629, 2009.

[7] D. Zulli, R. Alaggio, and F. Benedettini, "Non-linear dynamics of curved beams. Part 2, numerical analysis and experiments," *International Journal of Non-Linear Mechanics*, vol. 44, no. 6, pp. 630–643, 2009.

[8] F. Benedettini, R. Alaggio, and D. Zulli, "Nonlinear coupling and instability in the forced dynamics of a non-shallow arch: Theory and experiments," *Nonlinear Dynamics*, vol. 68, no. 4, pp. 505–517, 2012.

[9] A. H. Nayfeh, W. Kreider, and T. J. Anderson, "Investigation of natural frequencies and mode shapes of buckled beams," *AIAA Journal*, vol. 33, no. 6, pp. 1121–1126, 1995.

[10] W. Kreider and A. Nayfeh, "Experimental investigation of single-mode responses in a fixed-fixed buckled beam," *Nonlinear Dynamics*, vol. 15, pp. 155–177, 1998.

[11] A. H. Nayfeh, W. Lacarbonara, and C.-M. Chin, "Nonlinear normal modes of buckled beams: three-to-one and one-to-one

internal resonances," *Nonlinear Dynamics*, vol. 18, no. 3, pp. 253–273, 1999.

[12] W. Lestari and S. Hanagud, "Nonlinear vibration of buckled beams: Some exact solutions," *International Journal of Solids and Structures*, vol. 38, no. 26-27, pp. 4741–4757, 2001.

[13] S. A. Emam and A. H. Nayfeh, "Nonlinear Responses of Buckled Beams to Subharmonic-Resonance Excitations," *Nonlinear Dynamics*, vol. 35, no. 2, pp. 105–122, 2004.

[14] A. H. Nayfeh and S. A. Emam, "Exact solution and stability of postbuckling configurations of beams," *Nonlinear Dynamics*, vol. 54, no. 4, pp. 395–408, 2008.

[15] S. A. Emam and A. H. Nayfeh, "Non-linear response of buckled beams to 1:1 and 3:1 internal resonances," *International Journal of Non-Linear Mechanics*, vol. 52, pp. 12–25, 2013.

[16] S. A. Emam and M. M. Abdalla, "Subharmonic parametric resonance of simply supported buckled beams," *Nonlinear Dynamics*, vol. 79, no. 2, pp. 1443–1456, 2014.

[17] P. Ribeiro and R. Carneiro, "Experimental detection of modal interaction in the non-linear vibration of a hinged-hinged beam," *Journal of Sound and Vibration*, vol. 277, no. 4-5, pp. 943–954, 2004.

[18] J. L. Huang, R. K. L. Su, Y. Y. Lee, and S. H. Chen, "Nonlinear vibration of a curved beam under uniform base harmonic excitation with quadratic and cubic nonlinearities," *Journal of Sound and Vibration*, vol. 330, no. 21, pp. 5151–5164, 2011.

[19] S. Maleki and A. Maghsoudi-Barmi, "Effects of Concurrent Earthquake and Temperature Loadings on Cable-Stayed Bridges," *International Journal of Structural Stability and Dynamics*, vol. 16, no. 6, 2016.

[20] G. Y. Wu, "The analysis of dynamic instability and vibration motions of a pinned beam with transverse magnetic fields and thermal loads," *Journal of Sound and Vibration*, vol. 284, no. 1-2, pp. 343–360, 2005.

[21] G.-Y. Wu, "The analysis of dynamic instability on the large amplitude vibrations of a beam with transverse magnetic fields and thermal loads," *Journal of Sound and Vibration*, vol. 302, no. 1-2, pp. 167–177, 2007.

[22] E. Manoach and P. Ribeiro, "Coupled, thermoelastic, large amplitude vibrations of Timoshenko beams," *International Journal of Mechanical Sciences*, vol. 46, no. 11, pp. 1589–1606, 2004.

[23] P. Ribeiro and E. Manoach, "The effect of temperature on the large amplitude vibrations of curved beams," *Journal of Sound and Vibration*, vol. 285, no. 4-5, pp. 1093–1107, 2005.

[24] X.-X. Guo, Z.-M. Wang, Y. Wang, and Y.-F. Zhou, "Analysis of the coupled thermoelastic vibration for axially moving beam," *Journal of Sound and Vibration*, vol. 325, no. 3, pp. 597–608, 2009.

[25] F. Treyssède, "Vibration analysis of horizontal self-weighted beams and cables with bending stiffness subjected to thermal loads," *Journal of Sound and Vibration*, vol. 329, no. 9, pp. 1536–1552, 2010.

[26] J. Avsec and M. Oblak, "Thermal vibrational analysis for simply supported beam and clamped beam," *Journal of Sound and Vibration*, vol. 308, no. 3–5, pp. 514–525, 2007.

[27] M. H. Ghayesh, S. Kazemirad, M. A. Darabi, and P. Woo, "Thermo-mechanical nonlinear vibration analysis of a spring-mass-beam system," *Archive of Applied Mechanics*, vol. 82, no. 3, pp. 317–331, 2012.

[28] H. Farokhi and M. H. Ghayesh, "Thermo-mechanical dynamics of perfect and imperfect Timoshenko microbeams," *International Journal of Engineering Science*, vol. 91, pp. 12–33, 2015.

[29] A. Warminska, E. Manoach, and J. Warminski, "Nonlinear dynamics of a reduced multimodal Timoshenko beam subjected to thermal and mechanical loadings," *Meccanica*, vol. 49, no. 8, pp. 1775–1793, 2014.

[30] A. Warminska, E. Manoach, J. Warminski, and S. Samborski, "Regular and chaotic oscillations of a Timoshenko beam subjected to mechanical and thermal loadings," *Continuum Mechanics and Thermodynamics*, vol. 27, no. 4-5, pp. 719–737, 2015.

[31] V. Settimi, E. Saetta, and G. Rega, "Local and global nonlinear dynamics of thermomechanically coupled composite plates in passive thermal regime," *Nonlinear Dynamics*, vol. 93, no. 1, pp. 167–187, 2018.

[32] E. Saetta, V. Settimi, and G. Rega, "Nonlinear vibrations of symmetric cross-ply laminates via thermomechanically coupled reduced order models," *Procedia Engineering*, vol. 199, pp. 802–807, 2017.

[33] Y. Zhao, Z. Wang, X. Zhang, and L. Chen, "Effects of temperature variation on vibration of a cable-stayed beam," *International Journal of Structural Stability and Dynamics*, vol. 17, no. 10, 1750123, 18 pages, 2017.

[34] Y. Zhao, J. Peng, Y. Zhao, and L. Chen, "Effects of temperature variations on nonlinear planar free and forced oscillations at primary resonances of suspended cables," *Nonlinear Dynamics*, vol. 89, no. 4, pp. 2815–2827, 2017.

[35] Y. Zhao, C. Huang, L. Chen, and J. Peng, "Nonlinear vibration behaviors of suspended cables under two-frequency excitation with temperature effects," *Journal of Sound and Vibration*, vol. 416, pp. 279–294, 2018.

[36] E. Özkaya, M. Pakdemirli, and H. R. Öz, "Non-liner vibrations of a beam-mass system under different boundary conditions," *Journal of Sound and Vibration*, vol. 199, no. 4, pp. 679–696, 1997.

[37] M. Amabili, "Nonlinear vibrations of rectangular plates with different boundary conditions: theory and experiments," *Computers & Structures*, vol. 82, no. 31-32, pp. 2587–2605, 2004.

[38] A. Mamandi, M. H. Kargarnovin, and S. Farsi, "An investigation on effects of traveling mass with variable velocity on nonlinear dynamic response of an inclined Timoshenko beam with different boundary conditions," *International Journal of Mechanical Sciences*, vol. 52, no. 12, pp. 1694–1708, 2010.

[39] S. Lenci, F. Clementi, and J. Warminski, "Nonlinear free dynamics of a two-layer composite beam with different boundary conditions," *Meccanica*, vol. 50, no. 3, pp. 675–688, 2015.

[40] A. Luongo, G. Rega, and F. Vestroni, "On nonlinear dynamics of planar shear indeformable beams," *Journal of Applied Mechanics*, vol. 53, no. 3, pp. 619–624, 1986.

[41] Y. Xia, B. Chen, S. Weng, Y.-Q. Ni, and Y.-L. Xu, "Temperature effect on vibration properties of civil structures: a literature review and case studies," *Journal of Civil Structural Health Monitoring*, vol. 2, no. 1, pp. 29–46, 2012.

[42] Y. Zhao, C. Sun, Z. Wang, and L. Wang, "Approximate series solutions for nonlinear free vibration of suspended cables," *Shock and Vibration*, vol. 2014, Article ID 795708, 12 pages, 2014.

[43] Y. Zhao, C. Sun, Z. Wang, and L. Wang, "Analytical solutions for resonant response of suspended cables subjected to external excitation," *Nonlinear Dynamics*, vol. 78, no. 2, pp. 1017–1032, 2014.